SHOCK, Vol. 57, No. 4, pp. 544–552, 2022

OPEN

RECOMBINANT ACTIVATED PROTEIN C (RHAPC) AFFECTS LIPOPOLYSACCHARIDE-INDUCED MECHANICAL COMPLIANCE CHANGES AND BEAT FREQUENCY OF MESC-DERIVED CARDIOMYOCYTE MONOLAYERS

Aysegül Temiz Artmann,[*] Eylem Kurulgan Demirci,[*†] Ipek Seda Fırat,[*] Hakan Oflaz,[‡] and Gerhard M. Artmann[*]

[*]Institute for Bioengineering, University of Applied Sciences Aachen/Campus Juelich, Juelich, Germany; [†]Department of Chemistry, Faculty of Science, Izmir Institute of Technology, Campus Gulbahce, URLA, Izmir, Turkey; and [‡]Bioengineering Department, Faculty of Engineering, Gebze Technical University, Kocaeli, Turkey

Received 31 May 2021; first review completed 17 Jun 2021; accepted in final form 3 Aug 2021

ABSTRACT—**Background:** Septic cardiomyopathy increases mortality by 70% to 90% and results in mechanical dysfunction of cells. **Methods:** Here, we created a LPS-induced *in-vitro* sepsis model with mouse embryonic stem cell-derived cardiomyocytes (mESC-CM) using the CellDrum technology which simultaneously measures mechanical compliance and beat frequency of mESCs. Visualization of reactive oxygen species (ROS), actin stress fibers, and mRNA quantification of endothelial protein C receptor (EPCR) and protease-activated receptor 1 (PAR1) before/after LPS incubation were used for method validation. Since activated protein C (APC) has cardioprotective effects, samples were treated with human recombinant APC (rhAPC) with/-out LPS predamage to demonstrate the application in therapeutic studies. **Results:** Twelve hours LPS treatment (5 μg/mL) increased ROS and decreased actin stress fiber density and significantly downregulated EPCR and PAR1 compared to control samples (0.26, 0.39-fold respectively). rhAPC application (5 μg/mL, 12 h) decreased ROS and recovered actin density, EPCR, and PAR1 levels were significantly upregulated compared to LPS predamaged samples (4.79, 3.49-fold respectively). The beat frequencies were significantly decreased after 6- (86%) and 12 h (73%) of LPS application. Mechanical compliance of monolayers significantly increased in a time-dependent manner, up to eight times upon 12-h LPS incubation compared to controls. rhAPC incubation increased the beat frequency by 127% (6h-LPS) and 123% (12h-LPS) and decreased mechanical compliance by 68% (12h-LPS) compared to LPS predamaged samples. **Conclusion:** LPS-induced contraction dysfunction and the reversal effects of rhAPC were successfully assessed by the mechanical properties of mESC-CMs. The CellDrum technology proved a decent tool to simulate sepsis *in-vitro*.

KEYWORDS—Actin cytoskeleton, cardiomyocyte biomechanics, cardioprotection, CellDrum, EPCR, septic cardiomyopathy, LPS

INTRODUCTION

The World Health Organization (WHO) declared sepsis a global health priority, with an estimated 48.9 million cases worldwide in 2017, and has called for a resolution to improve the prevention, diagnosis, and management of this life-threatening disease (1). Sepsis, being a systemic inflammatory response, is the most common cause of death due to the dysfunction of several organs (2). The largest contributors of sepsis are bacterial endotoxins, especially LPS released by gram-negative bacteria (3). If not compensated, this infection causes severe disease symptoms in patients which in turn lead to excessive stimulation of the immune system and often fatal endotoxin shock (2). Rapid activation of the immune system results in the release of cytokines TNF-α, IL-6, and IL-1 beta (2). These cytokines contribute to the containment of infection by promoting several pathways including oxidation, production of nitric oxide and reactive oxygen species (ROS), activation of tissue factors, and coagulation cascade (2, 4). Collectively, these responses may injure endothelial cells by initiating clotting and inflammation and thus resulting in endothelial dysfunction. The endothelial dysfunction, in turn, causes microvascular thrombosis, which later leads to sepsis-induced cardiac dysfunction or septic cardiomyopathy (SCM) (5, 6). Septic cardiomyopathy (SCM) is an acute but reversible complication of sepsis-associated cardiovascular

Address reprint requests to Aysegül Temiz Artmann, Prof. Dr. med. (TR) Dr. Ph.D., Institute for Bioengineering, University of Applied Sciences Aachen, Campus Juelich, Heinrich-Mußmann-Str. 1, 52428 Juelich, Germany.
E-mail: a.artmann@fh-aachen.de

ATA and EKD contributed equally to this publication.

This work was financially supported by two R&D research grants to Prof. Dr. ATA from the BMWi (VP2425601AB9) and BMBF-AiF (1760X07). There was private-personal patent protection for the CellDrum technology (39–41). This patent was never nationalized because no investor/company could be found. Therefore, the patent protection was abandoned as of 2010 and its subject matter has been free for use by anyone since then.

ATA wrote and submitted the research proposals to fund the Ph.D. student EKD and CellDrum development. She wrote and edited the paper, directed the experimental part of the research, and supervised her Ph.D. students.

EKD was a Ph.D. student, she conducted much of the laboratory work, and wrote the rough text of the paper.

ISF: Ph.D. student, significant intellectual and scientific contribution to the up-to-date evaluation of the results, literature, and manuscript.

HO: Biomechanist, contributed to the work of EKD with extensive discussions and experimental planning.

GMA: Invented the CellDrum technology with his Ph.D. students, advised on the acquisition of research proposals to fund CellDrum development, and advised on the writing of the paper.

The authors report no conflicts of interest.

DOI: 10.1097/SHK.0000000000001845

insufficiency (5–7). When combined with sepsis, SCM is known to increase mortality by 70% to 90% (5). The contractile dysfunction of the heart in SCM is the most serious and frequently observed symptom. It often results in dilatation of the ventricles accompanied by the enlargement of the heart, decreased contractility, hypotension, vascular hyporeactivity, impaired myocardial compliance, as well as reduced ejection fraction (5, 8–11).

Protein C, a natural anticoagulant, is a vitamin K-dependent zymogen found readily in blood plasma (12). Upon activation, together with thrombin and thrombomodulin, activated protein C (APC) is known to downregulate the coagulation process (12–14). Aside from anticoagulant action, APC was shown to have cytoprotective, anti-inflammatory, and anti-apoptotic effects (15, 16). APC protects endothelial cell barrier through endothelial protein C receptor (EPCR) dependent protease-activated receptor 1 (PAR 1) cleavage-induced upregulation of sphingosine-1-phosphate (S1P), simultaneously inhibits the release of inflammatory cytokines (IL-1β, IL-6, and TNF-α), downregulates cell surface adhesion molecules (such as ICAM-1, VCAM-1, and E-selectin), and by activation of Rac1 signaling compensates the destructive effects of the RhoA signaling pathway as well as downregulates apoptotic genes like p53 and Bax (15–18). Anti-apoptotic effects of APC were observed not only for endothelial cells but also for cardiomyocytes (CM). In a mouse model of acute reperfusion injury (I/R) it was shown that administration of APC represses the acute ischemic injury of the heart by stimulating activated protein kinase (AMPK) and inhibiting nuclear factor-κB (NF-κB) and c-Jun N-terminal kinase (JNK) signaling pathways, which are closely related to anticoagulant action (17). Further, the established presence of EPCR on CMs and the triggering of AMPK pathways accentuated the possibility of the cardio-protective functions of APC (13, 17). It was shown that due to CM injury the serum troponin levels are elevated in patients with severe sepsis or septic shock, which is an indication of the deterioration and impaired beating of the heart tissue (19). A possible positive inotropic impact of APC on CMs was also suggested, which may involve the PAR1-cardiac troponin I (CTI) pathway (13, 20). Similarly, the reduction of APC levels was seen in sepsis patients either due to malfunctioning of the production/synthesis pathways, severe degradation, or down-regulation of EPCR and APC-related mechanisms and is also suggested as a prognostic parameter for sepsis (21, 22). Consequently, APC in recombinant form, human recombinant APC (rhAPC), was suggested as a therapeutic agent for sepsis and septic shock to improve the survival of patients with elevated troponin, cardiomyopathy, and microvascular disturbances (20, 23, 24). In this sense, rhAPC was used in several prospective observational or randomized, placebo-controlled studies throughout the past two decades (24, 25). The most famous randomized studies PROWESS (Recombinant human Activated Protein C Worldwide Evaluation in Severe Sepsis) and PROWESS-SHOCK (almost 10 years apart) revealed conflicting, not-reproducible however incomparable results (25, 26). Most of the studies conducted were focused on anti-inflammatory and anticoagulant functions of rhAPC and not on its effects on CMs and contractility. Therefore, the need for more trials, and especially, when possible, personalized experiments in the context of sepsis were highlighted and are still the foci of many studies (26–28).

Although there exists no universal consensus or method, *in-vitro* sepsis models have been the main setting used for sepsis, sepsis-induced complications, and drug development and testing studies. Many of the models mainly involve animals (murine, canine) or human subjects, where sepsis/septic shock are induced by injection or direct delivery of bacteria (such as *Streptococcus pneumonia*), Endotoxin (such as LPS), and human septic shock serum, all of which involve invasive manipulation of the subjects (29, 30). Another experimental model used to simulate septic-environment is achieved through utilization of animal or human cells *in-vitro*, which is less invasive, and additionally can be used to assess the tissue/cell-specific responses. Till now, cardiac force measurements were carried out either by invasive techniques with animal/human models and tissue sections or via edge-recognition and microscopic observations using cultured cell monolayers (20, 31). Previously, we conducted a study on contractile properties of human aortic endothelial cells in an LPS-induced sepsis model using the CellDrum technology (32). The CellDrum technology, which has been developed in our laboratory, enables the cultivation of cell monolayers on thin (approximately 4 μm), biocompatible and elastic silicon membranes bound to plastic rings which allow free movement of cell monolayer (33–38). Simultaneously, the mathematical reciprocal value of cell-monolayer mechanical compliance, which corresponds to cardiac beat frequency, can be determined via a device housing a displacement sensor.

An LPS-induced reduction of force generation and transmission, which *in vivo* corresponds to a relaxation of the heart muscle (cardiac dysfunction), was previously shown for murine cardiomyocytes (31). In this paper, we report the advantageous and successful application of the CellDrum technology and its feature to directly quantify the mechanical compliance (mechanical tension) of cell monolayers and to use LPS *in-vitro* as a first step toward developing a sepsis model based on this technique. We assess LPS-induced damage on the cultured CMs with five seemingly rather unconnected measurement techniques (RT-qPCR technique), microscopic imaging, mechanical compliance, and beat frequency as an attempt to widen the technological scope of solving biological and medical questions.

The CellDrum creates an appropriate environment for disorder simulations, drug testing, and assessment of the mechanical behavior of cells. LPS exposure caused contraction dysfunction of CMs which was measured by beat frequency and mechanical compliance. After LPS application ROS generation increased, whereas gene expression of EPCR and PAR1, and actin cytoskeleton density decreased. rhAPC incubation of cells following LPS-treatment inhibited the detrimental effects of LPS on the actin cytoskeleton, gene expression, and mechanical behavior.

MATERIALS AND METHODS

Cell culture

For the experiments, mouse embryonic stem cell (mESC)-derived cardiomyocytes were obtained from Lonza, Germany (Cat. No. XCAC-1010E Cor.At 1 M GFP mESC, Axiogenesis). The cells were stored in liquid nitrogen until

used. The mESC culture medium (Cat. No. XCAM-250E mESC Complete Culture Medium) and puromycin stock solution were thawed, following the instructions, at 4°C overnight. Puromycin was added to the cell culture medium at a final concentration of 10 μM. Puromycin was used as a selection agent and phenotype indicator.

As mentioned, our main purpose here was to provide a new LPS-induced sepsis/cardiac dysfunction model of cardiomyocytes using the CellDrum technology which enables us to follow beating frequency and compliance quantification. The CellDrum was patented by Gerhard M. Artmann in 2000 and used since then in our laboratory as an experimental device on which this publication is based (39–41). The PDMS membranes are made in our laboratory using a Sylgard 184 silicone elastomer kit. Membrane thicknesses are measured interferometrically followed by a chemical-biological functionalization process. Tunable protein/gel coating enables good cell attachment for the desired cultured cells on CellDrums (34, 35, 38).

The cells were seeded in 300 μL complete medium on the fibronectin-coated polydimethylsiloxane (PDMS) membrane (membrane thickness 4 μm, culture area 2.01 cm^2) with a density of 100,000 cells/cm^2. CellDrum PDMS membranes were coated with 1% Fibronectin in MES buffer prior to seeding. The puromycin-containing Cor.at medium is required for medium change after 24 h of plating and the first 3 days of culture. After day 4 of culture Cor.at medium without puromycin was used and the medium was changed every other day. All samples were routinely checked for bacterial or fungal contamination using standard microscopic methods whereas the polymerase chain reaction (PCR) amplification method (VenorGeM, BIOCHROM AG, Berlin, Germany) was used to check for mycoplasma contamination. The results were negative for contamination. The cells were used only at the first passage and a maximum of 7 days without passaging. Cell morphology and monolayer confluence were checked every 12 h. The cells reached confluence after 2 days of culture on CellDrum membranes.

Lipopolysaccharide preparation

Lipopolysaccharide (LPS) derived from *E. coli* was acquired from Sigma, Germany (LPS 055: B5; Cat. No. L2880). LPS was diluted in sterile Dulbecco's phosphate-buffered saline (DPBS). To enable extended storage, small volumes of the LPS stock solutions were frozen at −20°C. Before application, the LPS solution was thawed and shaken at room temperature for about 30 min to prevent the deposition of LPS on the tube's surface. After thawing, the solution was stored at +8°C until use and kept sterile.

Recombinant human activated protein C (rhAPC) preparation

The recombinant human-activated protein C (rhAPC) was obtained from Eli Lilly and Company in May 2009 (pre-withdrawal, Cat. No. LY203638). It was diluted in sterile distilled water in glass-free vials and stored at −80°C. According to the company's instructions, the suggested dose of rhAPC to mimic physiological conditions was 5 μg/mL.

LPS stimulation of the mESC-CMs

To determine the suitable LPS concentration dose-response and time-course experiments were previously carried out using cardiac endothelial cells (32). The study groups were formed in concentrations 0.1 μg/mL, 0.5 μg/mL, 1 μg/mL, and 2 μg/mL. The IL-6 protein level was checked by ELISA and the biggest increase was seen in samples treated with 0.5 μg/mL LPS. Therefore, to create a uniform sepsis model and to better assess the LPS in circulation rather than tissue-accumulated, a dose of 0.5 μg/mL LPS was chosen to stimulate mESC-CMs as well. After reaching 80% confluence the cells were washed with complete medium and 0.5 μg/mL LPS was mixed with the fresh complete medium. Control samples were incubated with the complete medium only.

Treating the mESC-CMs with rhAPC (after LPS stimulation)

After 30 min of LPS (0.5 μg/mL) application, the cell medium was renewed, and the cells were incubated with 5 μg/mL rhAPC for 12 hours (h) at 37°C. Four experiment groups were created: Control, 12 h LPS-treatment, 12 h rhAPC-treatment following 12 h LPS treatment, 12 h rhAPC-treatment mESC-CMs. All groups had six replicates. The control samples were incubated only with the complete medium.

Real-time quantitative PCR (RT-qPCR)

Total RNA was extracted (RNeasy mini kit, Qiagen, Cat. No: 74106) from cardiomyocytes which were used as a template for cDNA synthesis. QuantiTect reverse transcription kit (Qiagen, Cat. No: 205311) was used to transcribe RNA into cDNA. Real-time quantitative PCR was performed with BIORAD iCycler device. 18sr RNA and GAPDH RNA genes were used as housekeeping genes. Primers (22) were purchased from Qiagen Company (18 s (Qiagen, Hs_RRN18S_1_SG QuantiTect Primer Assay (200), Cat. No.: QT00199367), F2r (PAR1) (Mm_F2r_1_SG QuantiTect Primer Assay (200), Cat. No.: QT0119812), Procr (EPCR) (Mm_Procr_1_SG QuantiTect Primer Assay (200), Cat. No.: QT00103061)).

ROS visualization and confocal microscopy

3'-(p-hydroxyphenyl) fluorescein (HPF) (Molecular Probes, Cat. No. H36004) was used as an indicator for highly reactive oxygen species. The 3'-(p-hydroxyphenyl) fluorescein stock solution was diluted in Dulbecco's modified Eagle medium (DMEM). After the completion of LPS and rhAPC treatments cells were incubated with the diluted HPF solution for 10 min at room temperature and washed to remove the excess probe and replaced with fresh buffer. The pictures were taken under a confocal laser scanning microscope (LSM 510, Zeiss, Oberkochen, Germany) with a ×20 objective lens (LD-Achroplan, Zeiss) using the integrated data processing software (LSM 3.0, Zeiss).

Actin stress fiber visualization and confocal microscopy

After reaching confluence, cells were treated either with LPS, rhAPC, or both as previously explained. Samples were washed twice with prewarmed DPBS, fixed with 3.7% formaldehyde for 15 min at room temperature. Cell membranes were penetrated using 0.1% Triton-X 100 for 5 min. The samples were washed thrice with DPBS and the actin cytoskeleton was stained with 2% Alexa Fluor 488 phalloidin (Invitrogen, Cat. No. A12379) in DPBS for 20 min at room temperature. The samples were washed thoroughly with DPBS and imaged using a confocal laser scanning microscope (LSM 510, Zeiss, Oberkochen, Germany) with a ×20 objective lens (LD-Achroplan, Zeiss) using the integrated data processing software (LSM 3.0, Zeiss).

Beat frequency and mechanical compliance measurements

Cardiomyocyte beat frequency and mechanical compliance were determined simultaneously with the help of the CellDrum technology and an experimental setup. Together with the cell monolayer, the PDMS membrane forms a ''mechanically coupled double-layer'' membrane. Having thickness values of 4 μm, the PDMS membranes, therefore, have known and high mechanical compliance, which depends on the force development and transmission of the cell monolayer. The overall compliance of the double-layer thus is determined solely by the mechanical tensile forces and their transmission within the cell monolayer. By slowly increasing the pressure under the membrane and simultaneously measuring the resulting membrane deflection, sigmoid pressure-deflection curves are created. The strain/stress (mechanical compliance) is then calculated by simple conversion of the slope at zero crossings. The membrane deflection is measured by the laser system (LK-031, KEYENCE GmbH, Neu-Isenburg, Germany) (33, 37, 38). When cells contract, the length of the membrane shortens, resulting in an increasing proportion of strain/pressure. In relation to the contractile tension results, this represents an indirect ratio between cellular contraction and the strain applied to the membrane. Strain, as deformation per unit length, is calculated as shown in the formula below;

$$\varepsilon = \delta l \div l \tag{1}$$

ε: Strain in measured direction δl: Original length of the material l: Change in the length of the material h: Deflection of the membrane

Here, to understand the fold change differences between groups, the reciprocal of normalized strain/pressure results were used. The data were collected and processed via a custom LabVIEW software (National Instruments, Austin, Tex).

When CMs reached confluence, they started beating synchronously. The cells were then stimulated with 0.5 μg/mL LPS for 3 h, 6 h, and 12 h. In addition, after the completion of LPS treatment samples were incubated with 5 μg/mL rhAPC for another 12 h. Records of synchronously beating CMs were made, and LabVIEW software was used to evaluate frequency changes of cells before and after LPS and/or rhAPC application, respectively. Each experimental group had six samples. Every sample was measured three times.

Statistical analysis

Experiments were carried out with six replicates. The beat frequency and mechanical compliance were measured three times for descriptive statistical

analysis. All data were analyzed with Sigma Stat for Windows, version 3.5. Comparison of more than two groups was carried out with a two-way analysis of variance followed by the Wilcoxon Rank Sum test, with significance defined as $P < 0.05$.

RESULTS

rhAPC reverses the LPS downregulated EPCR (Procr) and PAR1 (F2r) mRNA levels

The RT-qPCR results indicated that mRNA levels of Procr and F2r were significantly downregulated after 12-h exposure of 0.5 μg/mL LPS by 0.26- and 0.39-fold, respectively, when compared with the control groups. Conversely, rhAPC application after LPS-induced cell damage resulted in increased expressions of Procr and F2r significantly when compared with LPS-treated samples (4.79- and 3.49-fold respectively) which indicates a recovery effect of rhAPC application (Fig. 1). The application of rhAPC alone seemed to reduce EPCR mRNA expression compared with the control group; however, this reduction was shown to be not significant.

LPS increases ROS whereas rhAPC inhibits ROS production

It is a well-established fact that ROS production increases during sepsis and ROS mediates contraction dysfunction in cardiomyocytes (42, 43). ROS production was monitored with HPF staining of CMs. 12 h LPS-treated samples showed stronger brightness when compared to control samples (Fig. 2, A and B). In contrast, the brightness diminished after rhAPC application as seen in Figure 2C. rhAPC application alone did not cause a visible difference when compared to control samples (Fig. 2, A and D).

LPS decreases actin stress fiber density

To show the morphological changes of cell cytoskeletal response to LPS treatment we investigated the presence and density of actin stress fibers via actin staining with phalloidin and confocal microscopy (Fig. 2, E–H). Control samples had a dense actin-filament network (Fig. 2 E) whereas upon 12 h LPS exposure (Fig. 2F) reduction in actin cytoskeleton density was observed. Confocal microscopic analysis of actin fibers of LPS- and rhAPC-treated samples (Fig. 2G) demonstrated somewhat a betterment in actin density when compared to LPS-treated samples and were almost visually indistinguishable from the control samples. On the other hand, no visible difference in actin stress fiber density was seen for only rhAPC-treated samples (Fig. 2H) compared to control samples.

LPS affect the beat frequency of CM monolayers

In this study, we determined the beating frequency of CMs after LPS, rhAPC application following LPS treatment, and in control samples with the help of CellDrum technology (Fig. 3). Figure 4 demonstrates the time-dependent decrease of cardiac beating frequency after 0.5 μg/mL LPS treatment. Compared to control groups, LPS significantly decreased cardiac beating frequency by 86% after 6 h and 73% after 12 h of LPS incubation. All in all, LPS alone caused a significant decrease in the beat frequency, but not yet significantly after 3 h.

On the other hand, the application of rhAPC to LPS predamaged CM monolayers resulted in a significant reversal of this beat frequency reduction. After rhAPC treatment following 6 h of LPS incubation, the beat frequency increased by 127% relative to the LPS damage level and tended to be approximately 5% higher than that of the control. After rhAPC

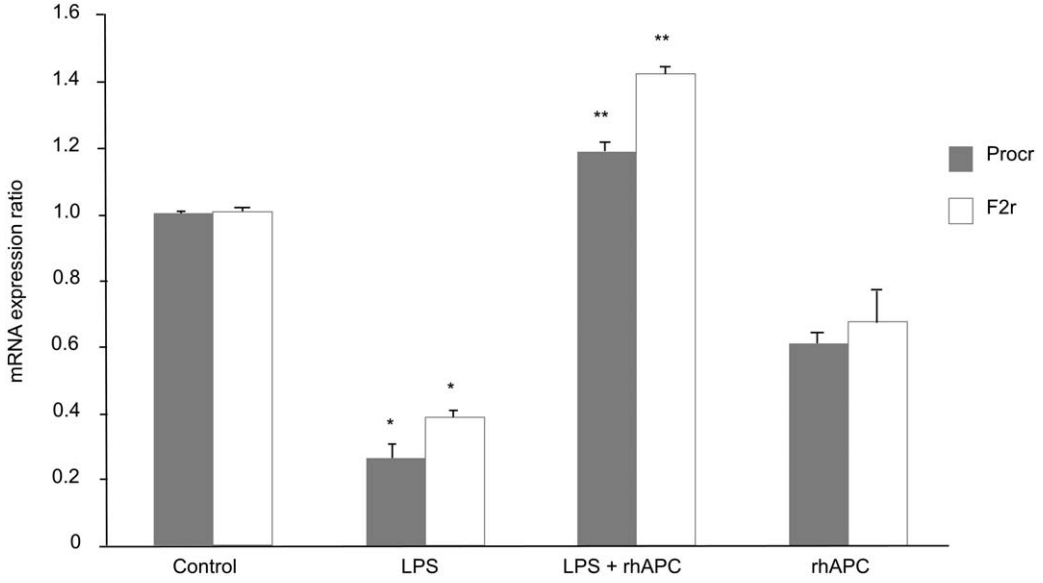

Fig. 1. **Effect of LPS and rhAPC on the expression of the mRNAs of mESC derived CMs (after 12 h exposure).** Procr codes for the endothelial protein C receptor (EPCR) and F2r codes for the protease-activated receptor-1 (PAR-1). Both mRNA levels were significantly decreased in the presence of LPS compared to controls. In LPS-damaged CM monolayers, Procr was reduced by 0.26- and F2r to 0.39 times, respectively. On the other hand, rhAPC application after LPS cell damage upregulated mRNA expression to 1.18-fold for Procr and 1.41-fold for F2r compared to controls. Both values were significantly increased under rhAPC compared to the effect of LPS alone (**). rhAPC alone showed no significant change (* $P < 0.05$ vs. control, ** $P < 0.01$ vs. LPS alone, rank-sum test, n = 6 for each condition).

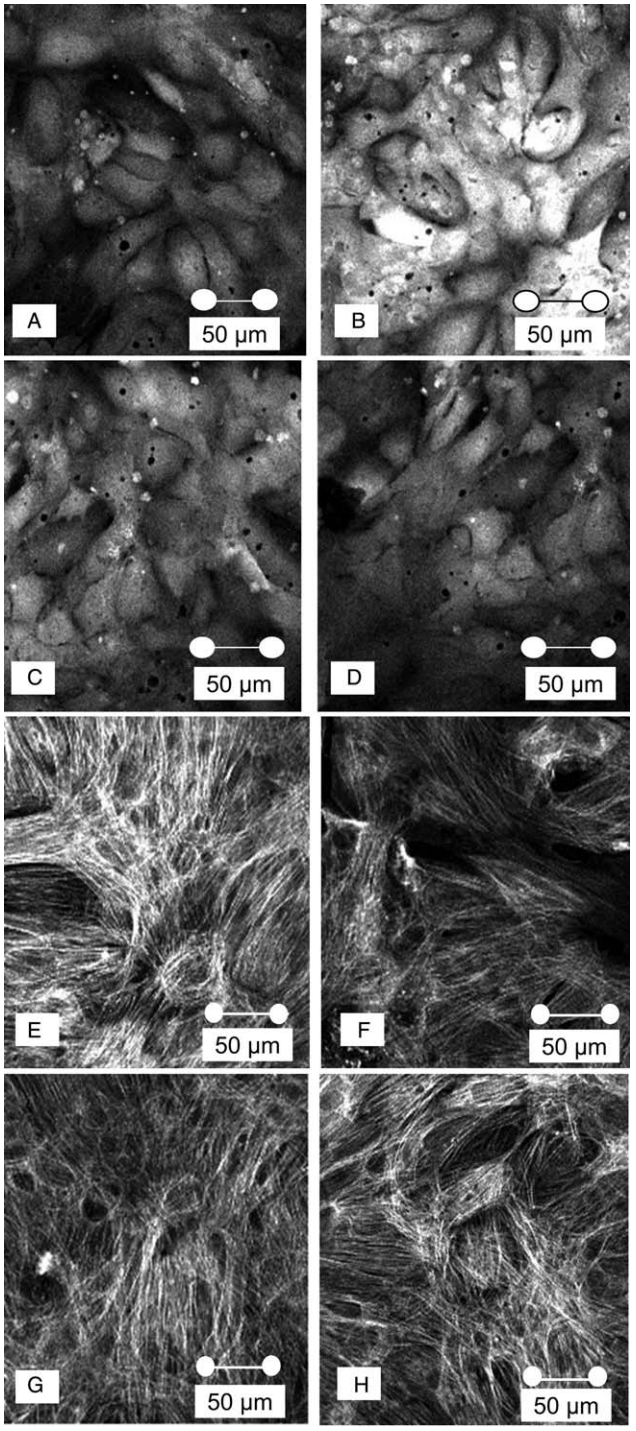

Fig. 2. **A–D, Fluorescence images of mESC-derived CM monolayers, control, and treatments after 12 h of LPS/rhAPC, respectively.** (A) Control, (B) with 0.5 µg/mL LPS 12 h, (C) with 5 µg/mL rhAPC after previous 12 h LPS exposure, and (D) with 5 µg/mL rhAPC alone. The CMs were stained with the fluorescent dye 3-(p-hydroxyphenyl) fluorescein (HPF), which is specific for highly reactive oxygen species. The controls (A) showed diminished fluorescence. The fluorescence signal rose sharply after LPS application, indicating stronger ROS activity (B) (bright white areas in the picture). ROS activity was diminished with rhAPC application after LPS damage (C) or with rhAPC alone (D). The photos were taken from cells on silicone membranes, and they are representative because similar pictures were found in six more replicas. E–H, Visualization of the actin cytoskeleton of mouse CMs. Confluent CM monolayers were stained with FITC Phalloidin and observed with confocal microscopically at (E) control, (F) with 0.5 µg/mL LPS 12 h, (G) with 5 µg/mL rhAPC after previous 12 h LPS exposure, and (H) with 5 µg/mL rhAPC alone. LPS alone (F) significantly reduced the stress fiber density. Cell-free areas in the monolayer were observed compared to control, to some extent. The addition of rhAPC after LPS damage (G) resulted in seemingly increased stress fiber density that was visually indistinguishable from the controls (E) as well as rhAPC alone (H). The photos were taken from CM monolayers cultivated on flexible silicone membranes.

treatment following 12 h of LPS incubation, the beat frequency was still increased by 123% compared to 12 h LPS-treated samples, but about 5% lower than the control samples. The mentioned shifts compared to the controls were not significant. There was no significant difference between samples that were only incubated with rhAPC and control samples. However, significant increases were also seen between rhAPC-treated samples and both 6 h and 12 h LPS-treated samples.

LPS affects the mechanical compliance of CM monolayers

The CellDrum technology (Fig. 3) was used to measure the mechanical compliance and beat frequency of self-exciting mESC-derived CM monolayers simultaneously. To examine the compliance response to LPS, different exposure times (3 h, 6 h, 12 h) were investigated. LPS stimulation caused a significant increase in mechanical compliance within 3 h to 12 h of incubation, steadily enhanced with increasing incubation time (Fig. 5). Furthermore, we found that rhAPC reduced these negative compliance effects of LPS on cardiomyocyte monolayers for all three incubation periods (3 h, 6 h, 12 h). Although after 12 h of LPS-incubation the compliance was up to eight times higher in comparison with control, after 12 h of rhAPC application CM compliance has significantly decreased to about 68% of the LPS damage. However, the compliance level achieved by rhAPC treatment still corresponds to about 5.4 times the compliance of controls measured without the LPS treatment. Similar tendencies were obtained for the incubation times 3 h and 6 h. The effect of rhAPC alone showed no significant change compared to controls (Fig. 5).

DISCUSSION

Sepsis is a disorder characterized by hypotension, multiple organ dysfunction, and impaired cardiac contractility (2, 4–9). SCM is one of the clinical complications of sepsis and septic shock, which is distinguished by ventricular dilatation combined with impaired ventricular contractility and changes in stroke frequency, which are collectively related to the mechanobiological properties of cells (2, 4–9). Multiple molecular mechanisms and pathways underlying diseases, which may be used for diagnostic and therapeutic purposes, are very complex. On the contrary, the mechanical properties of cells can give direct information regarding the response to diseases and syndromes, such as sepsis, as well as possible treatment methods (20, 31). Although the novel CellDrum system is a relatively new method, it enables the routine, high accuracy measurement of the mechanical cell contraction and tension. We have confirmed the reliability of this measuring system in our previous studies (33–38). As described, there is an indirect ratio between contraction and strain in the CellDrum system. When the cells contract, the membrane shortens, and strain increases. This phenomenon is used to quantify cell

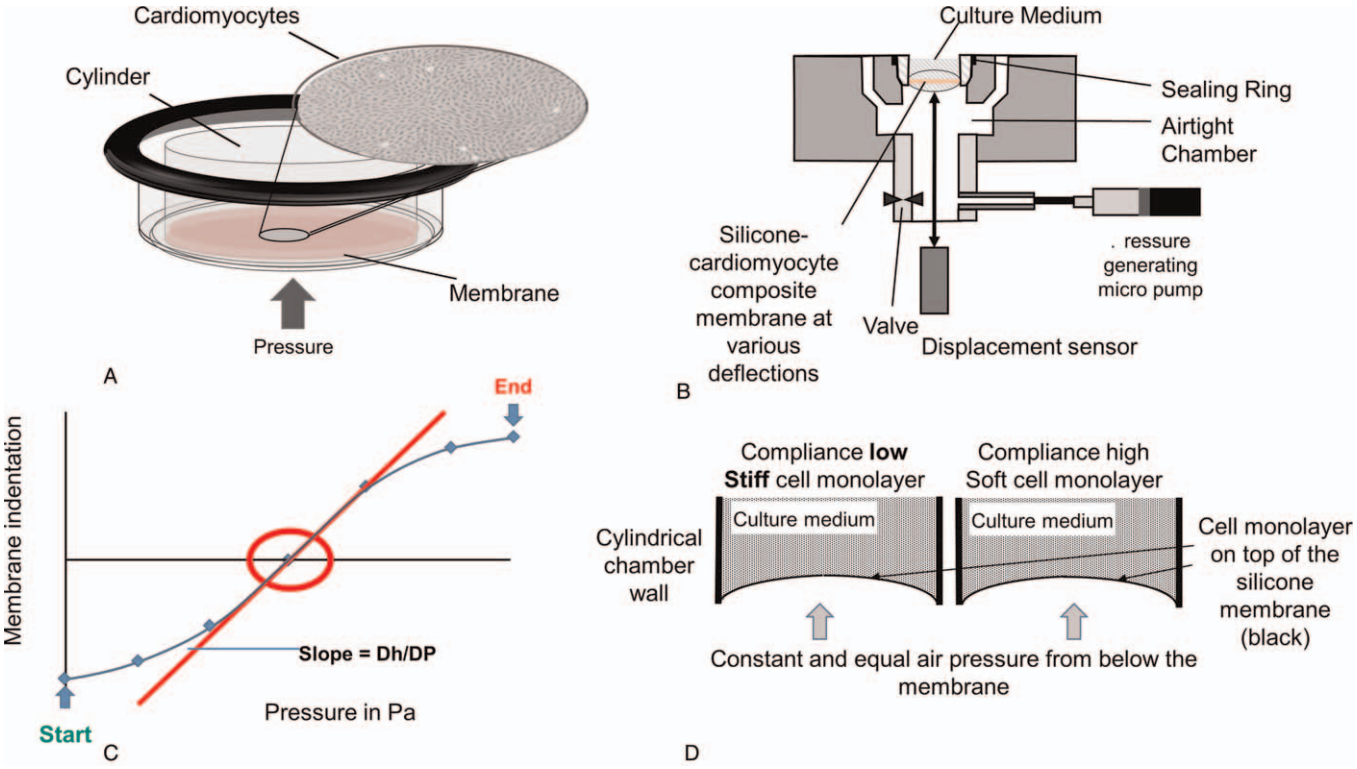

FIG. 3. **A–D, The CellDrum measuring principle: Method for measuring the mechanical compliance of confluent cell monolayers, here mouse embryonic stem cell (mESC) induced cardiomyocytes, which were cultured on a silicone membrane, were used.** (A) Single CellDrum setup, (B) setup for mechanical loading of the membrane (orange) with lower-end positions (start) and upper-end position, (C) scheme of a typical pressure to membrane-indentation/deflection graph. Data points with regression curve (blue), slope/tangent at zero crossing (red), (D) scheme of the pressure to membrane-indentation/deflection graphs (at the same pressure under the membrane). The membrane is a compound-membrane consisting of a 4-μm-thick PDMS to which mESC derived cardiomyocyte monolayer adheres; (left) stiff cell layer; (right) soft cell layer (cytoskeleton/intercellular bonds are weak).

contraction. The contraction and tension measurement of human aortic endothelial cells (HAoEC) monolayers cultivated on the CellDrum membranes under the influence of drugs that are known to cause contraction stress were performed (32). Furthermore, it was seen that cardiomyocytes cultivated on the CellDrums reach synchronized beating and cause rhythmic membrane deflection rapidly, and the CellDrum provides an environment in which cell biomechanics, therapeutic agents,

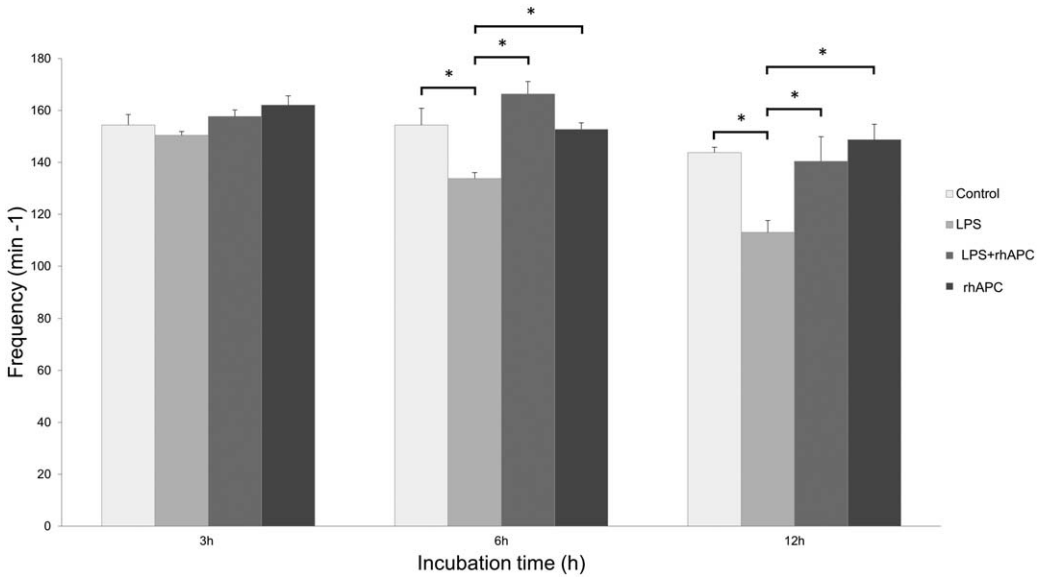

FIG. 4. **Time dependence of the beat frequency of the mESC-derived CM monolayer of control samples, 0.5 μg/mL LPS-treated samples over 3 h, 6 h, and 12 h, 5 μg/mL rhAPC application after previous treatment with 0.5 μg/mL LPS over 3 h, 6 h or 12 h, or with 5 μg/mL rhAPC alone, respectively (* $P < 0.05$, rank-sum test, six replicates, error bar as SEM).**

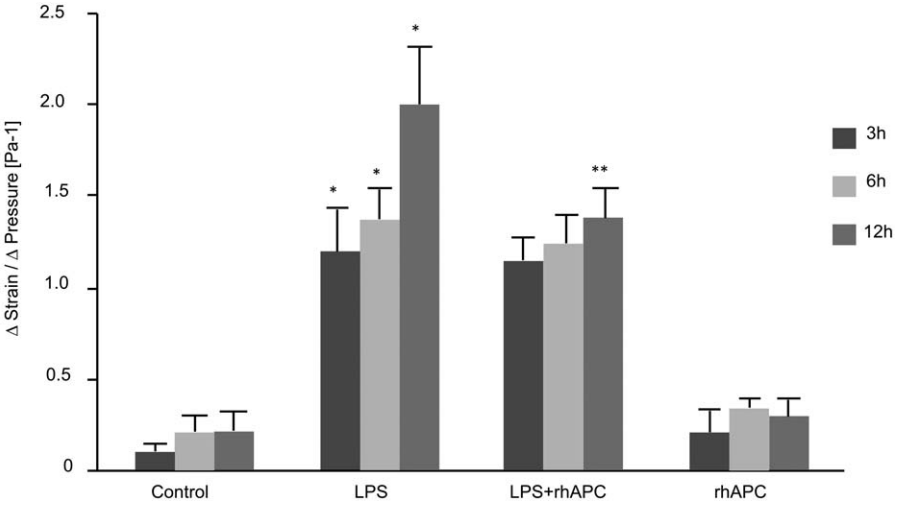

FIG. 5. **Mechanical compliance = ΔStrain/ΔPressure of the mESC-derived CM monolayer at incubation times 3 h, 6 h, and 12 h.** The mechanical compliance of the composite membrane silicone with CM monolayer is high if the cell monolayer is soft, i.e., pliable, at the same inflation pressure under the membrane. The following tests were performed at the times shown in the figure: controls, 0.5 μg/mL LPS-treatment, 0.5 μg/mL LPS, and subsequent application of 5 μg/mL rhAPC, and rhAPC alone. With LPS, CM monolayer compliances were significantly increased for all three incubation periods (*). After 12 h of LPS incubation, it was up to eight times higher. After 12 h rhAPC application, however, CM compliance had significantly decreased to about 68% of the previous damage (**). However, the compliance level achieved by rhAPC treatment still corresponds to about 5.4 times the compliance of controls measured before LPS treatment (*, ** $P < 0.05$, rank-sum test, six replicates, * significance versus control, ** significance between 12 h after LPS and 12 h + rhAPC).

and disease models could successfully be tested (33, 35, 36). Thus, in this study to better understand the biomechanical responses of CM monolayers and to establish an *in-vitro* LPS-induced sepsis model we used the ''CellDrum'' technology. For the assessment of the LPS-induced damage the real-time PCR technique (Fig. 1), microscopic methods (Fig. 2) were used, mechanical compliance (Fig. 4), and beat frequency (Fig. 5) were measured with the help of the CellDrum system.

In-vitro results from the literature already state the LPS-induced downregulation of mRNA levels for EPCR and PAR1 (22, 44). In this model, we have verified these effects in CMs by real-time qPCR (Fig. 1). Figure 1 shows that LPS reduces the levels of EPCR mRNA in cardiomyocytes after 12 h of LPS incubation. The incubation period of 12 h was chosen to allow enough time because of the slow development of gene expression, and, on the other hand, the number of samples could not be increased for technical reasons. Therefore, in future studies, a time-course analysis of EPCR mRNA expression would be informative after LPS addition. LPS-induced downregulation of EPCR and PAR1 was partially reversed after APC application which further accentuates the aforementioned cytoprotective and anti-inflammatory responses to APC. Since this study was planned on the gene expression level, the relevant protein determination should remain part of the future studies. Affymetrix microarray analysis, bridging with specific proteins will enlighten the underlying mechanism in future work.

Further, it is well known that ROS production increases during sepsis, and in this study, the detrimental effects of LPS were shown microscopically through increased ROS production after 12-h LPS exposure. Yet again after APC administration, the ROS-induced fluorescence diminished, as shown in Figure 2A–D, which emphasizes the anti-inflammatory action of APC.

The actin cytoskeleton has a fundamental role in various cellular processes and the most important physiological function of actin filaments is to produce force, which generates cell contraction tension (45). These results on actin stress fibers content in cardiomyocytes support the beat frequency and mechanical compliance results as well (Figs. 4 and 5). Cardiomyocytes exposed to LPS exhibit less actin stress filaments since LPS causes cytoskeletal damage (46, 47). This correlates with the data shown in Figure 2E–H, which demonstrates decreased stress fiber density in LPS-treated samples and again partial inhibition of the damaging effect of LPS by APC application.

Several studies stated that in *in-vitro* conditions LPS causes cardiac dysfunction and a decrease in cardiac contractility while ROS mediates the contraction dysfunction (31, 42, 46). We showed that LPS increases mechanical compliance and decreases beat frequency (Figs. 4 and 5). The increase in mechanical compliance due to LPS exposure (Fig. 5) can be colloquially referred to as *in-vitro* mechanical weakening of the cells. This weakening can be supported again by the decrease in F-actin stress fiber density, shown in Figure 2, which is also accompanied by the reduction in beat frequency (Fig. 4) and increased cell strain. Moreover, APC incubation of LPS predamaged cells inhibits the effects of LPS to some extent by increasing beat frequency and decreasing mechanical compliance (Figs. 4 and 5). These results can also be substantiated by mRNA expression experiments of EPCR and PAR1 (Fig. 1). Previous studies showed that APC regulates the contractility of cardiomyocytes via the EPCR and PAR1 pathways (15–17, 48). Ultimately, partial normalization of ROS production (Fig. 2, A–D), actin cytoskeleton density (Fig. 2, E–H), beat frequency (Fig. 4), and mechanical compliance (Fig. 5) after APC treatment supports the notion that APC has anti-inflammatory and

inotropic effects of on CMs. The correlation between the cardiomyocyte mechanical deformation (compliance) and the beat frequency is known and in *in-vitro* studies, the same observations are expected (49–51). As the calcium effect on cardiomyocyte frequency is a well-established fact, the mechanical compliance and tissue integrity through actin dynamics and intercalated disc functions would be regulated by calcium changes in cardiomyocytes (49–51). Thus, we recommend using the CellDrum technology combined with calcium imaging techniques such as with Fura fluorescent dyes. Moreover, because of the important role of Rac1 and RhoA mechanisms as well as ROS in cellular health, actin dynamics and many more, relevant future studies bridging LPS and APC functioning in this context could help better understand the mechanism and possible other receptors (17, 52).

Here, for the first time, we showed the experimental setup of the CellDrum technique that can be successfully used in an LPS-induced *in-vitro* sepsis model for cardiomyocytes. We assessed LPS-induced damage on cultured CMs combining five seemingly rather unconnected measurement techniques to widen the technological scope for biologists, physiologists, and medical researchers solving biological and medical questions with bioengineering solutions. An extension and full automation of the CellDrum technique is nearing completion. At the end of 2021, the CellDrum technology including different CellDrum types will be commercially available (NPI Electronic GmbH, Tamm, Germany). This technology will also work for isolated primary neonatal and adult cardiomyocytes, respectively. In addition to the mechanical compliance and the beat frequency, individual contraction–relaxation cycles of CM monolayers could be analyzed with respect to the beat force amplitude, its temporal progression, its frequency, and its time integral. The results presented here indicate that the CellDrum technology is very promising in following cardiomyocyte *in-vitro* mechanical properties in basic and applied research.

Some limitations should be noted regarding the experiments. Although mESC-derived cardiomyocytes are used to evaluate responses *in-vitro*, it should be remembered that there are physiological differences when compared to human cardiomyocyte cells. The mechanisms underlying the observed differences in the experimental groups were not determined; therefore, further studies are required to understanding the pathophysiological mechanisms involved in LPS-induced stress and the beating capability of CMs. Moreover, it would be beneficial to perform time-course protein quantification for EPCR, PAR1, and other mentioned receptor proteins which would provide more insight into APC and LPS effects on CMs.

Overall, our principal aim here was to demonstrate new CellDrum technology features and the possible utilization in pathophysiological conditions partially modeling sepsis *in vitro* using LPS. This might serve as a basis for more complex modeling systems for sepsis.

ACKNOWLEDGMENTS

This research was carried out in the laboratories and by employees of the FH Aachen University of Applied Sciences. The authors thank all collaborating colleagues for their generous administrative and technical support to write this manuscript and encourage their research. The authors dedicate this article to Dr. Taylan Demirci, a man with a passion for biological science, especially genetics, who died very young.

REFERENCES

1. Rudd K, Johnson S, Agesa K, Shackelford K, Tsoi D, Kievlan D, Colombara D, Ikuta K, Kissoon N, Finfer S, et al.: Global, regional, and national sepsis incidence and mortality, 1990–2017: analysis for the Global Burden of Disease Study. *Lancet* 395(10219):200–211, 2020.
2. Delano M, Ward P: Sepsis-induced immune dysfunction: can immune therapies reduce mortality? *J Clin Invest* 126(1):23–31, 2016.
3. Opal SM: Endotoxins and other sepsis triggers. *Contrib Nephrol* 167:14–24, 2010.
4. Hotchkiss RS, Moldawer LL, Opal SM, Reinhart K, Turnbull IR, Vincent JL: Sepsis and septic shock. *Nat Rev Dis Primers* 2:16045, 2016.
5. Lin H, Wang W, Lee M, Meng Q, Ren H: Current status of septic cardiomyopathy: basic science and clinical progress. *Front in Pharmacol* 11:210, 2020.
6. Tsolaki V, Makris D, Mantzarlis K, Zakynthinos E: Sepsis-induced cardiomyopathy: oxidative implications in the initiation and resolution of the damage. *Oxid Med Cell Longev* 2017:7393525, 2017.
7. Beesley SJ, Weber G, Sarge T, Nikravan S, Grissom CK, Lanspa MJ, Shahul S, Brown SM: Septic cardiomyopathy. *Crit Care Med* 46(4):625–634, 2018.
8. Wang J, Wang XT, Liu DW, Zhang HM, Su LX: Induction and deduction in sepsis-induced cardiomyopathy: five typical categories. *Chin Med J (Engl)* 133(18):2205–2211, 2020.
9. L'Heureux M, Sternberg M, Brath L, Turlington J, Kashiouris MG: Sepsis-induced cardiomyopathy: a comprehensive review. *Curr Cardiol Rep* 22(5):35, 2020.
10. Habimana R, Choi I, Cho HJ, Kim D, Lee K, Jeong I: Sepsis-induced cardiac dysfunction: a review of pathophysiology. *Acute Crit Care* 35(2):57–66, 2020.
11. Fernandes CJ Jr, de Assuncao MS: Myocardial dysfunction in sepsis: a large, unsolved puzzle. *Crit Care Res Pract* 2012:896430, 2012.
12. Loubele S, Spek C, Leenders P, van Oerle R, Aberson H, Hamulya?k K, Ferrel G, Esmon CT, Spronk HMH, ten Cate H, et al.: Activated Protein C protects against myocardial ischemia/reperfusion injury via inhibition of apoptosis and inflammation. *Arterioscler Thromb Vasc Biol* 29(7):1087–1092, 2009.
13. Wang J, Yang L, Rezaie AR, Li J: Activated protein C protects against myocardial ischemic/reperfusion injury through AMP-activated protein kinase signaling. *J Thromb Haemost* 9(7):1308–1317, 2011.
14. Mosnier L, Zlokovic B, Griffin J: The cytoprotective protein C pathway. *Blood* 109(8):3161–3172, 2006.
15. Griffin J, Fernàndez J, Gale A, Mosnier L: Activated protein C. *J Thromb Haemost* 5:73–80, 2007.
16. Feistritzer C, Riewald M: Endothelial barrier protection by activated protein C through PAR1-dependent sphingosine 1–phosphate receptor-1 crossactivation. *Blood* 105(8):3178–3184, 2005.
17. Ren D, Giri H, Li J, Rezaie AR: The cardioprotective signaling activity of activated protein C in heart failure and ischemic heart diseases. *Int J Mol Sci* 20(7):1762, 2019.
18. Cheng T, Liu D, Griffin JH, Fernández JA, Castellino F, Rosen ED, Fukudome K, Zlokovic BV: Activated protein C blocks p53-mediated apoptosis in ischemic human brain endothelium and is neuroprotective. *Nat Med* 9(3):338–342, 2003.
19. Zochios V, Valchanov K: Raised cardiac troponin in intensive care patients with sepsis, in the absence of angiographically documented coronary artery disease: a systematic review. *J Intensive Care Soc* 16(1):52–57, 2015.
20. Alhamdi Y, Wang G, Toh C-H: Activated protein C (APC) and thrombin modulate cardiomyocytes contractility via a protease activated receptor-1 (PAR1)-cardiac troponin I (CTI) pathway. *J Thromb Haemost* 11:38–138, 2013.
21. Shorr AF, Bernard GR, Dhainaut JF, Russell JR, Macias WL, Nelson DR, Sundin DP: Protein C concentrations in severe sepsis: an early directional change in plasma levels predicts outcome. *Crit Care* 10(3):R92, 2006.
22. Levi M: Activated protein C in sepsis: a critical review. *Curr Opin Hematol* 15(5):481–486, 2008.
23. John J, Awab A, Norman D, Dernaika T, Kinasewitz GT: Activated protein C improves survival in severe sepsis patients with elevated troponin. *Intensive Care Med* 33:2122–2128, 2007.
24. Donati A, Damiani E, Botticelli L, Adrario E, Lombrano MR, Domizi R, Marini B, Van Teeffelen J, Carletti P, Girardis M, et al.: The aPC treatment improves microcirculation in severe sepsis/septic shock syndrome. *BMC Anesthesiol* 13:25, 2013.
25. Levi M, van der Poll T: Recombinant human activated protein C: current insights into its mechanism of action. *Crit Care* 11:S3, 2007.
26. Kalil AC, Florescu DF: Severe sepsis: are PROWESS and PROWESS-SHOCK trials comparable? A clinical and statistical heterogeneity analysis. *Crit Care* 17(4):167, 2013.
27. Eliézer S, de Figueiredo LFP, Colombari F: Prowess-shock trial. *Shock* 34(7):48–53, 2010.
28. Opal S, LaRosa S: Recombinant human activated protein C as a therapy for severe sepsis: lessons learned? *Am J Respir Crit Care Med* 187(10):1041–1043, 2013.

29. Fink MP: Animal models of sepsis. *Virulence* 5(1):143–153, 2014.
30. Kumar A, Brar R, Wang P, Dee L, Skorupa G, Khadour F, Schulz R, Parrillo JE: Role of nitric oxide and cGMP in human septic serum-induced depression of cardiac myocyte contractility. *Am J Physiol* 276(1):R265–R276, 1999.
31. Hobai IA, Morse JC, Siwik DA, Colucci WS: Lipopolysaccharide and cytokines inhibit rat cardiomyocyte contractility in vitro. *J Surg Res* 193(2):888–901, 2015.
32. Kurulgan Demirci E, Linder P, Demirci T, Trzewik J, Digel I, Artmann G, Temiz Artmann A: Contractile tension of endothelial cells: an LPS based in-vitro sepsis model. *IUBMB life* 61(3):307–308, 2009.
33. Artmann G. Device and method for the measurement of forces from living materials. Germany; EP1311850A1, 2000.
34. Trzewik J, Artmann-Temiz A, Linder PT, Demirci T, Digel I, Artmann GM: Evaluation of lateral mechanical tension in thin-film tissue constructs. *Ann Biomed Eng* 32(9):1243–1251, 2004.
35. Linder P, Trzewik J, Rüffer M, Artmann GM, Digel I, Kurz R, Rothermel A, Robitzki A, Temiz Artmann A: Contractile tension and beating rates of self-exciting monolayers and 3D-tissue constructs of neonatal rat cardiomyocytes. *Med Biol Eng Comput* 48(1):59–65, 2010.
36. Bayer R, Artmann AT, Digel I, Falkenstein J, Artmann G, Creutz T, Hescheler J: Mechano-pharmacological testing of L-Type Ca2+ channel modulators via human vascular celldrum model. *Cell Physiol Biochem* 54(3):371–383, 2020.
37. Trzewik J, Ates M, Artmann GM: A novel method to quantify mechanical tension in cell monolayers. *Biomed Tech (Berl)* 47(suppl 1 pt 1):379–381, 2002.
38. Artmann GM, Artmann A, Zhubanova A, Digel I. Functional toxicology and pharmacology test of cell induced mechanical tensile stress in 2d and 3d tissue cultures. Biological, Physical and Technical Basics of Cell Engineering. 13. Singapore: Springer Nature, 2018, 157–193.
39. Artmann G. Device and method for the measurement of forces from living materials. United States; US20040033482A1, 2000.
40. Artmann G. Device and method for the measurement of forces from living materials. Australia; AU7638401A, 2000.
41. Artmann G. Device and method for the measurement of forces from living materials. Canada; CA2420141A1, 2000.
42. Peoples JN, Saraf A, Ghazal N, Pham TT, Kwong JQ: Mitochondrial dysfunction and oxidative stress in heart disease. *Exp Mol Med* 51(12):1–13, 2019.
43. Moris D, Spartalis M, Spartalis E, Karachaliou GS, Karaolanis GI, Tsourouflis G, Tsilimigras DI, Tzatzaki E, Theocharis S: The role of reactive oxygen species in the pathophysiology of cardiovascular diseases and the clinical significance of myocardial redox. *Ann Transl Med* 5(16):326, 2017.
44. Zheng GJ, Wu ZX, Li YP, Yao YM: Effect of Xuebijing injection on expression of endothelial protein C receptor and protease activated receptor 1 mRNA and protein in endothelial cells induced by lipopolysaccharide. *Zhongguo Wei Zhong Bing Ji Jiu Yi Xue* 21(3):175–178, 2009.
45. Tojkander S, Gateva G, Lappalainen P: Actin stress fibers—assembly, dynamics and biological roles. *J Cell Sci* 125(Pt 8):1855–1864, 2012.
46. Llano-Diez M, Cheng A, Jonsson W, Ivarsson N, Westerblad H, Sun V, Cacciani N, Larsson L, Bruton J: Impaired Ca2þ release contributes to muscle weakness in a rat model of critical illness myopathy. *Crit Care* 20(1):254–261, 2016.
47. Wang L, Chen T, Zhou X, Huang Q, Jin C: Atomic force microscopy observation of lipopolysaccharide-induced cardiomyocyte cytoskeleton reorganization. *Micron* 51:48–53, 2013.
48. Kondreddy V, Wang J, Keshava S, Esmon CT, Rao LVM, Pendurthi UR: Factor VIIa induces anti-inflammatory signaling via EPCR and PAR1. *Blood* 131(21):2379–2392, 2018.
49. Cohen O, Safran S: Theory of frequency response of mechanically driven cardiomyocytes. *Sci Rep* 8(1):2237, 2018.
50. Antoons G, Mubagwa K, Nevelsteen I, Sipido K: Mechanisms underlying the frequency dependence of contraction and [Ca 2+] i transients in mouse ventricular myocytes. *J Physiol* 543(3):889–898, 2002.
51. Romero-Bermejo F, Ruiz-Bailen M, Gil-Cebrian JJ, Huertos-Ranchal M: Sepsis-induced cardiomyopathy. *Curr Cardiol Rev* 7(3):163–183, 2011.
52. Soh U, Trejo J: Activated protein C promotes protease-activated receptor-1 cytoprotective signaling through -arrestin and dishevelled-2 scaffolds. *Proc Natl Acad of Sci U S A* 108(50):E1372–E1380, 2011.